Journal of Oil Palm Research Vol. 37 (4) December 2025 p. 707-718
DOI: https://doi.org/10.21894/jopr.2024.0044

INVESTIGATION ON MECHANICAL AND CORROSION CHARACTERISTICS OF ASME SA 516 GRADE 70 CARBON STEEL USED IN A BIODIESEL STORAGE FACILITY

NUR NAQIUDDIN MDD NORDIN[1]*; MOHD NASHRUL MOHD ZUBIR[1]*; SALIM NEWAZ KAZI[1] and NURIN WAHIDAH MOHD ZULKIFLI[1]

ABSTRACT

In this experimental study, the impact of B100 biodiesel corrosion on the 15 years old ASME SA 516 Grade 70 carbon steel storage tank was investigated. This study provides novel insights into the material's performance and reliability of 15 years old ASME SA 516 Grade 70 carbon steel plate material under prolonged B100 biodiesel storage. Various analytical techniques, including ultrasonic thickness gauge measurements, scanning electron microscopy (SEM) and energy-dispersive X-ray spectroscopy (EDS), were used to assess corrosion behaviour and morphology. Tensile tests were conducted to evaluate the mechanical properties. The findings showed significant deterioration in both mechanical properties and corrosion resistance due to B100 biodiesel corrosion beyond the API 653 tolerance; hence, replacement is required to ensure mechanical integrity. The study also examines surface characteristics using SEM and EDS analyses, showing significant alterations in the metal's morphology and composition due to B100 biodiesel exposure. Additionally, the article discusses corrosion measurement and the remaining life of tanks, indicating a need for regular maintenance and repair. The mechanical performance of the steel is also assessed, showing a decrease in tensile strength and ductility. This indicates the potential risk B100 biodiesel corrosion poses to the carbon steel storage tank's performance and reliability.

Keywords: biodiesel corrosion, carbon steel storage tank, corrosion rate, mechanical properties, specific energy absorption.

Received: 6 November 2023**; Accepted:** 18 June 2024**; Published online:** 9 September 2024.

INTRODUCTION

Biodiesel is a type of fuel that has attracted much interest recently due to its lower carbon emissions and renewable nature (Aatola et al., 2009). The Malaysian government, through the Malaysian Palm Oil Board (MPOB), has stressed its commitment to be a carbon-neutral nation by 2050 and biodiesel will play a significant role in this direction. According to Parveez et al. (2021), in 2020, there were 20 operational oleochemical plants and 19 biodiesel plants in Malaysia, with processing capacities of 2.63 million tonnes and 2.23 million tonnes, respectively. The majority of these facilities are situated in Selangor and Johor, with eight oleochemical plants in Selangor, seven in Johor, and six biodiesel plants in each of these states. However, using biodiesel poses challenges in designing and maintaining storage tanks, particularly concerning corrosion. Biodiesel's corrosive properties are well documented in the literature (Kugelmeier et al., 2021). Biodiesel contains free fatty acids (FFA) and other compounds that can facilitate the formation of corrosive compounds, resulting in storage tank failures. Due to the formation of iron soaps and other corrosion products, carbon steel tanks, commonly used in storage tank construction, can exacerbate the corrosive nature of biodiesel (Rocha et al., 2019). The corrosive nature of biodiesel, more so than

[1] Department of Mechanical Engineering,
Faculty of Engineering,
University of Malaya,
50603 Kuala Lumpur, Malaysia.

* *Corresponding author e-mail: s2151766@siswa.um.edu.my; nashrul@um.edu.my*

traditional diesel, can lead to material degradation, sludge formation and microbial growth. While biodiesel offers benefits, its widespread use is hampered by several factors: Its high cost, potential competition with food resources, environmental concerns like deforestation for crop production, and technical issues such as fuel filter blockages and injector contamination. Additionally, biodiesel's lower oxidative stability makes it more prone to fuel oxidation and its reduced heating value affects engine performance in terms of torque and power. Its oxidative instability, poor performance in cold temperatures and solvent properties also contribute to its fewer desirable characteristics (Aatola et al., 2009; Bocha et al., 2007; Fazal et al., 2012; Gunstone, 2009; Samuel & Gulum, 2019).

The impact of biodiesel on storage tank integrity has been the subject of several previous studies. In a study conducted by Fazal et al. (2011), the authors examined the influence of biodiesel on the corrosion behaviour of carbon steel. Their investigation revealed that exposure to biodiesel led to elevated corrosion rates and the formation of iron soaps. The study also found that the corrosive properties of biodiesel were more severe at higher temperatures and in the presence of water. In a similar vein, a comprehensive investigation conducted by Kugelmeier et al. (2021) examined the corrosive properties of biodiesel on a range of storage tank materials, including carbon steel, stainless steel and aluminium. The study found that biodiesel exposure resulted in significant corrosion and pitting on all materials tested, with carbon steel being the most severely affected. Yung et al. (2018) investigated the compatibility of palm biodiesel blends (B7, B10 and B15) with automotive fuel tank materials, focusing on terne sheets. The research found that when high-quality fuels were used, palm biodiesel blends did not cause corrosion or compatibility issues with terne sheets, as demonstrated by scanning electron microscopy analysis and the absence of heavy metal leaching.

The mechanical properties of storage tanks can also be compromised by biodiesel corrosion. Corrosion can lead to reduced tensile strength, and hardness, increasing the risk of storage tank failures (Samuel & Gulum, 2019). Consequently, it is crucial to comprehensively assess the long-term performance of storage tanks by evaluating their mechanical properties when exposed to biodiesel. Furthermore, the impact of biodiesel corrosion on the fatigue behaviour of storage tanks remains an underexplored area, necessitating further research.

The literature also suggests several strategies to mitigate the effects of biodiesel corrosion on storage tanks. These include the use of corrosion inhibitors (Alam et al., 2022; Arunkumar et al., 2018; Atikpo et al., 2022; Chen & Sun, 2022; Diaz-Ballote et al., 2022; Fernandes et al., 2021a, 2021b; Jiang et al., 2019; Martins et al., 2020; Ouarga et al., 2022; Patil et al., 2018; Touazi et al., 2020; Yi et al., 2018). However, the effectiveness of these strategies may vary depending on the specific properties of the biodiesel and the storage tank materials. In addition, some of these strategies may have negative environmental impacts and may not be sustainable in the long run. Moreover, it is essential to consider the economic implications of biodiesel corrosion on storage tank maintenance and replacement costs. Storage tank failures due to biodiesel corrosion can lead to significant environmental, economic and safety consequences (Wei et al., 2021). Hence, there is a pressing need to develop cost-effective and sustainable strategies aimed at mitigating the harmful effects of biodiesel corrosion on storage tank integrity.

The impact of biodiesel on storage tank integrity has significant economic, environmental and safety implications. Storage tank failures can result in environmental damage, economic loss and threats to public safety. Therefore, it is critical to understand the mechanisms of biodiesel corrosion and to identify strategies to mitigate its effects. While previous studies have investigated the corrosive properties of biodiesel, there is still a need for more comprehensive studies that evaluate the mechanical properties of storage tanks exposed to biodiesel (Batista et al., 2019; Cursaru et al., 2018; Fernandes et al., 2019, 2021b; Kugelmeier et al., 2021; Martins et al., 2020; Pusparizkita et al., 2020; Serqueira et al., 2021). The mechanical properties of storage tanks can be compromised by corrosion, leading to reduced tensile strength, ductility, and fracture toughness. Therefore, it is crucial to evaluate the mechanical properties of carbon steel exposed to biodiesel to assess their long-term performance. This study aims to bridge this research gap by thoroughly investigating the corrosion and mechanical properties of carbon steel tanks exposed to biodiesel. The assessment will employ weight loss analysis and electrochemical tests to determine the corrosion rate of the tank. Tensile testing and hardness testing will be conducted before and after exposure to biodiesel to evaluate the mechanical properties of the tank. This study unveils comprehensive insights into the corrosion mechanisms affecting 15 years old ASME SA 516 Grade 70 carbon steel in B100 biodiesel in comparison to the virgin carbon steel plate, emphasising the critical importance of implementing tailored maintenance and inspection systems specific to industry and product requirements. The outcomes of this study will provide invaluable insights into the impact of B100 biodiesel storage on the performance and reliability of 15 years old ASME SA 516 Grade 70 carbon steel storage tanks.

MATERIALS AND METHODS

Carbon Steel

The carbon steel specimens utilised in this investigation were obtained from a tank that has been in service since 2007, conforming to the dimensions of 11.4 m outer diameter, 5.0 mm thickness and 7.2 m length, as represented in *Figure 1*. The storage tank is constructed from ASME SA 516 Grade 70 carbon steel, designed for a pressure of 19.2 bar and operating at 10.0 bar, with a design temperature of 50°C and an operating temperature of 40°C. The steel's chemical composition, as presented in *Table 1*, contributes to its mechanical properties, ensuring a well-balanced combination of strength, ductility and corrosion resistance suitable for the specified conditions. The specimens were cut from the corroded shell plate sized 20 x 20 mm in accordance with ASTM E8/E8M. Then, the sample testing was conducted using the Universal Testing Machine (UTM), the Instron 3800, with a load frame capacity of 300 kN. During the test, the specimen is loaded with tension until it fractures. The machine measures and records various data points, such as the force applied and the elongation of the specimen. The ultimate tensile strength (UTS), yield strength and elongation were calculated from these data.

TABLE 1. OPERATING DETAILS, MECHANICAL PROPERTIES AND CHEMICAL COMPOSITION FROM MANUFACTURER

Description	Details
Product	Palm oil methyl-ester (PME)
Year of service	2007-2023
Material	ASME SA 516 Grade 70
Design pressure	19.2 bar
Operating pressure	10.0 bar
Design temperature	50°C
Operating temperature	40°C
Parameters	**Values**
Yield strength (MPa)	345
Tensile strength (MPa)	510
Elongation (%)	28.5
Hardness (HRB)	76.5
Element	**Carbon steel (wt%)**
Carbon	0.200
Silicon	0.220
Manganese	0.430
Phosphorus	0.020
Sulphur	0.011
Chromium	0.160
Nickel	0.190
Copper	0.020
Molybdenum	0.001
Vanadium	0.010

The biodiesel employed in this study was obtained from a local biodiesel producer, and its chemical composition was determined using standardised test methods, as tabulated in *Table 2*.

Table 1 describes the biodiesel storage tank operating details and the mechanical properties of the ASME SA 516 Grade 70 carbon steel. Based on the parameters listed in *Table 2*, it can be concluded that monitoring and controlling water content, oxidative stability, sulphur content and acid value are essential to minimise the corrosive impact of biodiesel on carbon steel storage tanks. Extreme temperature fluctuations during storage can lead to condensation inside the storage tanks, introducing moisture into the palm oil methyl-ester (PME). If PME is stored in a humid environment or in containers that are not properly sealed, moisture can enter the biodiesel. Moisture can be introduced into the biodiesel through poor handling or storage conditions. Water can lead to the hydrolysis of the esters in the biodiesel, forming FFA, which can be corrosive. On the other hand, PME contains sulphur compounds, which can react with moisture during storage to form hydrogen sulphide and other corrosive sulphur-containing compounds. Furthermore, exposure to air can lead to oxidation of the unsaturated components in the biodiesel, forming peroxides and acids, which can be corrosive too. Moreover, in the presence of water and at certain temperatures, microbial growth can occur in stored PME. Microorganisms can produce acidic byproducts, leading to corrosion.

Scanning Electron Microscopy (SEM) and Energy-Dispersive X-ray Spectroscopy (EDS)

The morphology and composition of the corrosion products on the carbon steel specimens were examined using scanning electron microscopy (SEM) and dispersive X-ray spectroscopy (EDS). SEM and EDS are widely employed techniques for the examination and analysis of elemental surface components in samples related to corrosion studies. SEM examination allows for the visualisation of metal surface morphology, deposits and corrosion products, which can range from crystalline to amorphous. In this study, the SEM Zeiss Evo MA10 with medium resolution, a solid-state secondary electron detector and a backscattered electron detector were utilised for multi-sample inspections with a resolution of 100 nm. Prior to mounting the specimens on SEM stubs, they underwent a thorough cleaning process with acetone and subsequent drying. High-resolution field emission scanning electron microscopy (FESEM) was utilised to capture SEM images, while EDS analysis was conducted using an EDS detector attached to the microscope. EDS analysis provides valuable chemical information about the features

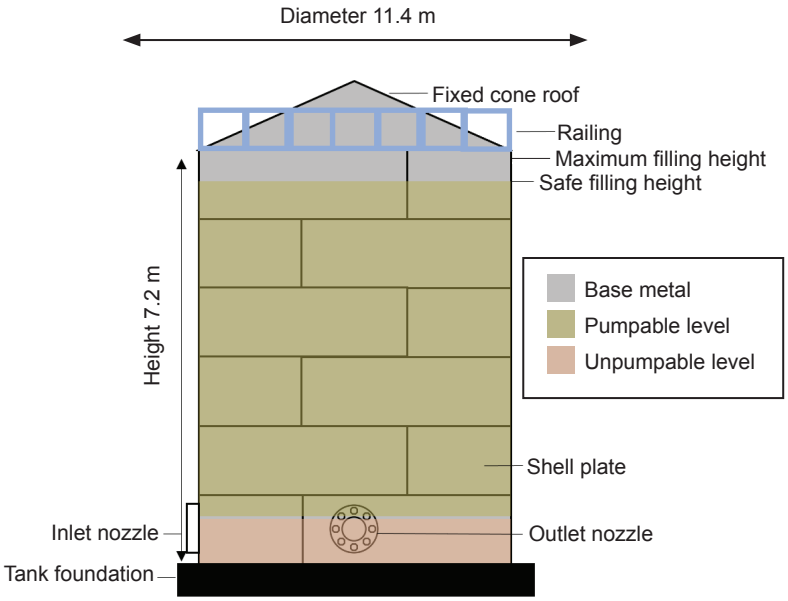

Figure 1. The biodiesel storage tank diagram and its dimension details.

TABLE 2. CHEMICAL COMPOSITION OF THE B100 PALM OIL METHYL-ESTER (PME) BIODIESEL USED IN THIS STUDY

Property	Unit	Limits		Test methods	Test result
		Min	Max		
Ester content	% (m/m)	96.5	-	EN 14103	99.7
Density @ 15°C	kg/m^3	860.0	900.0	ISO 3675	875.2
Viscosity @ 40°C	mm^2/s	3.500	5.000	ISO 3104	4.423
Flashpoint	°C	120	-	ISO 3679	150
Sulphur content	mg/kg	-	10.00	ISO 20846	<1.00
Cetane number	-	51.0	-	ISO 5165	72.1
Sulfated ash content	% (m/m)	-	0.020	ISO 3987	<0.001
Water content	mg/kg	-	500	ISO 12937	272
Total contamination	mg/kg	-	24	EN 12662	6
Copper strip corrosion (3 hr at 50°C)	Rating	-	1	ISO 2160	1a
Oxidation stability, 110°C	hr	10.0	-	EN 14112	23.5
Acid value	Mg KOH/g	-	0.50	EN 14104	0.25
Iodine value	g iodine/100 g	-	110.00	EN 14111	52.63
Linolenic acid methyl-ester	% (m/m)	-	12.0	EN 14103	0.10
Polyunsaturated methyl-esters (4 double bonds)	% (m/m)	-	1.00	EN 15779	<0.10
Methanol content	% (m/m)	-	0.20	EN 14110	0.03
Monoglyceride content	% (m/m)	-	0.70	EN 14105	0.51
Diglyceride content	% (m/m)	-	0.20	EN 14105	0.10
Triglyceride content	% (m/m)	-	0.20	EN 14105	0.01
Free glycerol	% (m/m)	-	0.020	EN 14105	0.019
Total glycerol	% (m/m)	-	0.25	EN 14105	0.17
Group I metal (Na + K)	mg/kg	-	5.000	EN 14108/14109	<1.000
Group II metals (Ca + Mg)	mg/kg	-	5.0	EN 14538	<1.0
Phosphorus content	mg/kg	-	4.0	EN 14107	<1.0
CFPP	°C	-	15	EN 116	+11

Source: Yusoff et al. (2021).

examined via SEM, enabling the identification and quantification of major, minor and trace elements present in the samples. SEM and EDS can provide valuable insights into the microstructure and chemistry of virgin and corroded samples.

Ultrasonic Thickness and Corrosion Rate Measurement

Ultrasonic testing thickness gauge (UTTG) is a non-destructive testing method commonly employed to determine the thickness of metals, including ship hulls, piping and structural steel. The method complies with ISO 9712 requirements at levels one, two and three (Purschke, 2013). The thickness range of the Olympus 45MG is 0.080-635.000 mm, the velocity range is 0.508-18.699 mm/s and the standard resolution is 0.010 mm. In many industries, software applications for monitoring corrosion, erosion and damage are critical. This technique calculates the round-trip transit time of an ultrasonic pulse from the gauge to the first back wall echo. By measuring the time, it takes for the pulse to travel through the material and reflect off the back wall, the gauge can determine the metal thickness. Based on this time interval and the speed of sound in the material, the thickness of the material can be calculated, as illustrated in *Figure 2*. Equation (1) was used to calculate the nominal thickness of the steel plate d_{steel}:

$$d_{steel} = \frac{V_{steel} \times t_{steel}}{2} \quad (1)$$

where, V_{steel} is the sound travel velocity (mm/μs), t_{steel} denotes the time required for the soundwave to return (μs). V_{steel} is computed into Equation (2) to calculate the corrosion rate, C_r (mm/yr).

$$C_r = \frac{d_0 - d_{steel}}{Yr} \quad (2)$$

where, d_0 represents the initial plate thickness (mm) and Yr denotes the duration of plate exposure with the service fluid (Years). On the other hand, minimum thickness of the plate, d_{min} (mm) is calculated using Equation (3):

$$d_{min} = \frac{66.04\,(H - 0.3)\,DG}{SE} \quad (3)$$

where, D is the steel rolling diameter, in feet (ft) while H is the plate length, in feet (ft). In tank design, G represents the highest specific gravity of the tank contents, S denotes the maximum allowable stress in lbf/in² and E signifies the original joint efficiency of the tank. The values for the parameters listed are presented in *Table 3*.

TABLE 3. THE STEEL ROLLING DIAMETER (D), THE HIGHEST SPECIFIC GRAVITY OF THE TANK CONTENTS (G), THE MAXIMUM ALLOWABLE STRESS (S), AND THE ORIGINAL JOINT EFFICIENCY OF THE TANK, (E)

Parameters	D (m)	G (kg/m³)	S (N/mm²)	E
Values	34.20	0.780	172	1.0

The C_r and V_{steel} are used to calculate the remaining life, RL (years) through Equation (4):

$$RL = \frac{d_{steel} - d_{min}}{C_r} \quad (4)$$

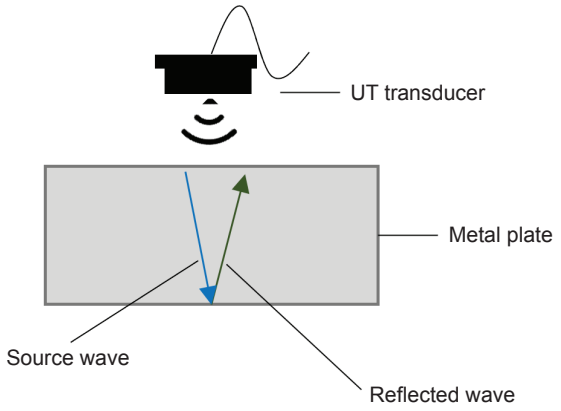

Figure 2. The schematic diagram of the working principle of UTTG.

Corrosion rate and remaining life calculations serve as valuable tools in assessing the current condition and future prognosis of carbon steel storage tanks. By measuring the corrosion rate and estimating the remaining life, the effectiveness of corrosion prevention and mitigation methods such as coating, cathodic protection and corrosion inhibitors can be evaluated. Moreover, one can also plan for maintenance, repair, or replacement activities based on the corrosion rate and remaining life data. This system can help optimise the operational cost and extend the service life of carbon steel storage tanks. The thickness values were taken at the top, middle and bottom locations to represent the tank's biodiesel exposure level.

Tensile Test

To assess its structural integrity and durability, it is critical to investigate the mechanical properties of a corroded steel plate immersed in biodiesel. Tensile, hardness, testing, fatigue, toughness and impact tests can all be used to characterise corroded

steel plates immersed in biodiesel. Strength, ductility, hardness, fatigue life, fracture toughness and impact resistance are all mechanical properties that can be measured on corroded steel plates using these methods. Throughout their service lives, storage tanks experience forces in the axial and hoop directions. The tangential or hoop stress acting on the wall thickness is observed, as shown in Equation (5) (Jerome & Ross, 1997).

$$\sigma_H = \frac{P}{A} = \frac{pDL}{2Lt} = \frac{pD}{2t} \quad (5)$$

where, L denotes the length of the cylindrical structure, D denotes the internal diameter, t denotes the wall thickness and p denotes the fluid pressure inside the structure. Equation (6) is used to determine the longitudinal stress (Jerome & Ross, 1997).

$$\sigma_A = \frac{P}{A} = \frac{\pi D^2 p}{4\pi Dt} = \frac{pD}{4t} \quad (6)$$

Combining Equation (3) and Equation (4), the hoop stress is greater than the axial stress. Hence, studying stress in the hoop direction compared to the axial direction is crucial. The outcomes of these tests provide valuable insights into the extent and severity of corrosion damage, the impact of corrosion on the mechanical behaviour of steel plates, as well as potential failure modes and mechanisms associated with corroded steel plates. ASTM E8 tensile testing was conducted, where the specimens were subjected to a UTM at a crosshead speed of 2 mm/min until failure occurred (Kardak & Sinclair, 2020). The stress-strain curves derived from the test results were utilised to determine various mechanical parameters, such as the yield point and tensile strength.

RESULTS AND DISCUSSION

These findings showed that exposing carbon steel tanks to B100 biodiesel caused significant corrosion and deterioration of mechanical properties. Weight loss analysis and electrochemical tests were used to assess the corrosion rate of the tanks. Weight loss analysis revealed a corrosion rate of 0.26 mm/yr, which is higher than the oil and gas industry's recommended maximum corrosion rate of 0.1 mm/yr for carbon steel tanks. The findings of this study are consistent with previous research on the corrosive properties of biodiesel (Dharma et al., 2023; Diaz-Ballote & Genesca, 2021; Nguyen & Vu, 2019; Samuel & Gulum, 2019). Biodiesel has been linked to a variety of corrosion processes, including uniform corrosion, pitting corrosion and stress corrosion cracking. The exact mechanism of biodiesel corrosion is unknown, but it is thought to be caused by the presence of water, oxygen, and FFA in biodiesel, which promote the formation of corrosive compounds.

Surface Characteristic

SEM can reveal the surface features of the samples, such as cracks, pits, scales, films, and deposits. There are iron (III) oxide deposits on the surface of the corroded specimen. As previously reported by Kugelmeier et al. (2021) and Fazal et al. (2018), the EDS analysis revealed the presence of carbon and oxygen at 64.11 wt% and 15.92 wt%, respectively, indicating the formation of corrosion products such as Fe_2O_3. This observation suggests that the material was exposed to a less corrosive environment with lower oxygen concentrations, indicating the resistance of carbon steel when in contact with biodiesel blends (Maru et al., 2009). By comparing the SEM images and EDS spectra of virgin and corroded samples, it can be inferred that the corrosion affects the morphology and composition of the samples. According to Fazal et al. (2013), the existence of fatty acid compounds, oxygen, and water content contributed to the higher degradation of the metal surface. As illustrated in *Table 4* and *Figure 3*, the element weights exhibited variations between the virgin and corroded samples. The decrease in the molecular weight of iron and oxygen ions corresponds to an increase in carbon content. This phenomenon can be attributed to the reduction in iron ion weight caused by the formation of rust, which is deposited as a thin layer on the corroded sample surface, as illustrated in *Figure 4*. The red dots represent the EDS spots from which the measurements, in *Table 4*, were taken. Following that, the weight of the element oxygen decreases because the sample is corroded due to oxidation, whereas the weight of carbon increases because the carbon chain is breaking down and forming more carbon chains [Equation (7)].

$$4Fe + 3O_2 + 2H_2O \longrightarrow 2Fe_2O_3.H_2O \quad (7)$$

This reaction explains that the virgin sample had 4 mol of Fe and 8 mol of O_2 before corrosion occurred. This explains why the virgin sample contains the least amount of each component in EDS. The corroded metal has 6 mol of Fe, and all the component values have increased, indicating that the layer of corrosion has occurred.

Corrosion Measurement and Remaining

As illustrated in *Figure 5* and *Table 5*, reading #2 constitutes the highest C_r of 0.322 mm/yr and has the lowest RL of 7.4 years. This finding can be

TABLE 4. THE WEIGHT AND ATOMIC PERCENTAGE COMPARISON IN BETWEEN VIRGIN AND CORRODED SPECIMENS

Item	Virgin		Corroded	
	Weight (%)	Atomic (%)	Weight (%)	Atomic (%)
C	14.05	29.04	64.11	72.54
O	29.55	45.87	15.92	13.52
Fe	56.40	25.08	11.67	8.35

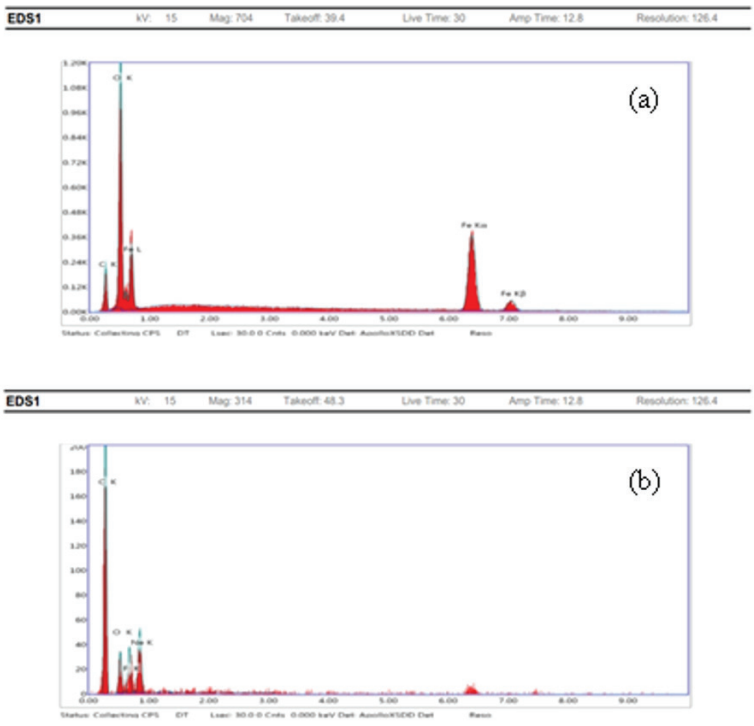

Figure 3. The EDS analysis of the (a) virgin, and (b) corroded specimens.

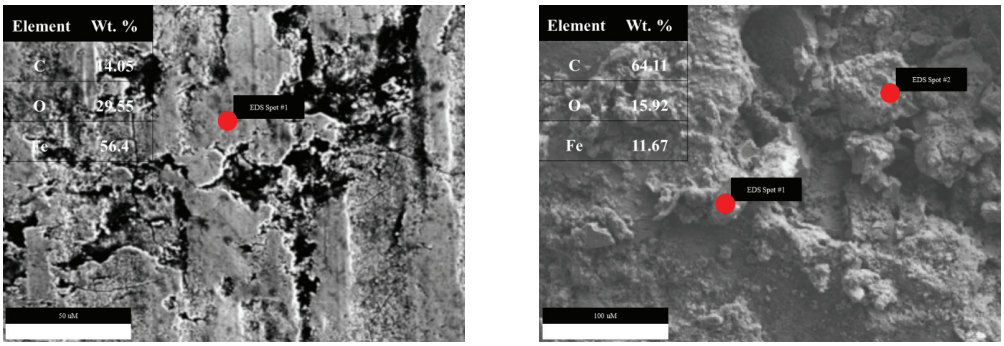

(a) Virgin (b) Corroded

Figure 4. The SEM images of (a) virgin, and (b) corroded samples after exposure to B100 biodiesel for 15 years.

attributed to the total exposure of the biodiesel throughout the service life. Compared to other shell courses, the first shell course has complete immersion and exposure at an unpumpable level, which contains the deadstock. As the biodiesel product is highly hygroscopic, water formation will settle at the bottom level of the first shell course. This finding aligns with the research conducted by Komariah et al. (2021), which investigated the corrosion behaviour of steel tanks upon contact with palm-based biodiesel. Their study focused on the corrosion type and behaviour in different zones within the fuel tank, with varying coating elements. The primary outcomes highlighted

those tanks made with various protective layers exhibited distinct types of corrosion, and the potential for leaks was higher at the base compared to the walls and roof of the storage tank. The increased corrosion rate observed in various metals in palm biodiesel can be attributed to the presence of oxygen and moisture absorption. Palm biodiesel typically contains 10-12 wt% oxygen, whereas conventional diesel does not contain oxygen. These findings are consistent with previous studies on the corrosion of metals in palm oil-based biodiesel blends conducted by (Fazal et al., 2019; Sgroi et al., 2005). As per API 653:2014, a storage tank must be externally inspected at least once every five years and internally inspected at least once every 20 years (American Petroleum Institute, 2014). Maintenance and repair should be conducted based on the corrosion rate (CR) and remaining life (RL) of the tank. This requirement aligns with Malaysia's Customs Act 1967, which mandates that subsidised storage tanks, including those for biodiesel products, must be calibrated within a 15 year duration (Parliament of Malaysia, 1967). Since readings #1 and #2 have remaining life durations lower than 15 years, the shell plate is required to be replaced.

Mechanical Performance

As presented in *Figure 6* and *Table 6*, the elastic region for the virgin specimen was maintained up to the yield point. However, the corroded specimen likely had a lower modulus of elasticity, as indicated by a reduced slope due to the changes in thickness and microstructure. The tensile test results showed that the yield point of the corroded specimens decreased by 30% compared to the virgin specimens, indicating that the corroded specimen begins to plastically deform at a lower stress level. The tensile strength decreased by 38%, indicating a compromised strength through a loss of ductility and toughness. The corroded sample also had a higher elongation at break than the virgin sample, suggesting that the material underwent plastic deformation before fracture. This finding is consistent with the observation that the material becomes more ductile after corrosion, meaning it can stretch further before breaking despite the loss of tensile strength. The finding is comparable to the finding by Samuel and Gulum (2019), which indicated that the brass tensile strength after exposure to B100 biodiesel for 960 hr was 70.77%.

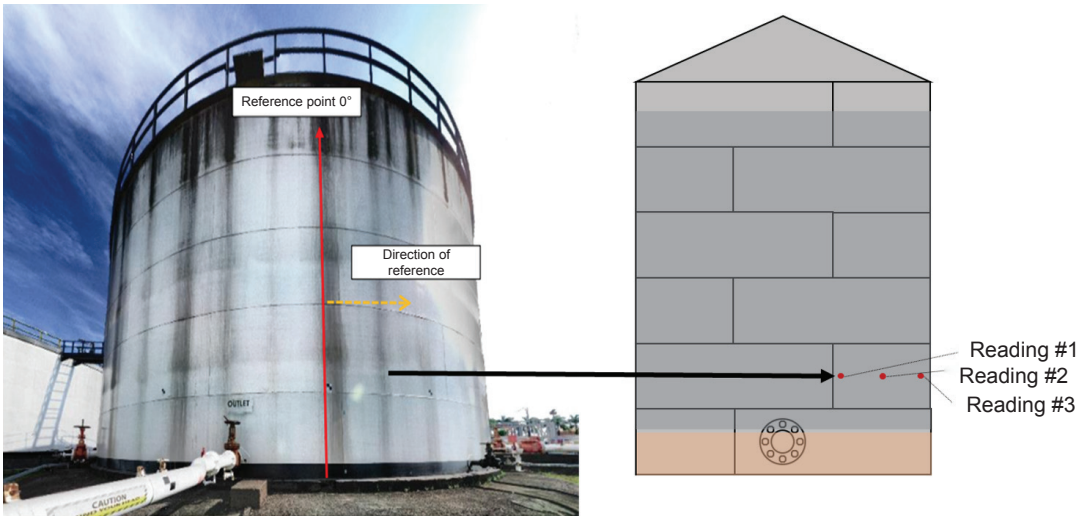

Figure 5. The illustration of the B100 biodiesel tank and its diagram showcasing the reading points.

TABLE 5. THE LOCATION READINGS AND THEIR INITIAL THICKNESS, MEASURED THICKNESS, MINIMUM THICKNESS, CORROSION RATE AND REMAINING LIFE

Reading	Initial thickness, d_0 (mm)	Measured thickness, d_{steel} (mm)	Minimum thickness, d_{min} (mm)	Corrosion rate, C_r (mm/yr)	Remaining life, RL (yr)
#1	7.11	5.61	2.80	0.2503	11.20
#2	7.11	5.18	2.80	0.3220	7.40
#3	7.11	6.08	2.80	0.1720	19.10
Average	7.11	5.62	2.80	0.2481	12.57

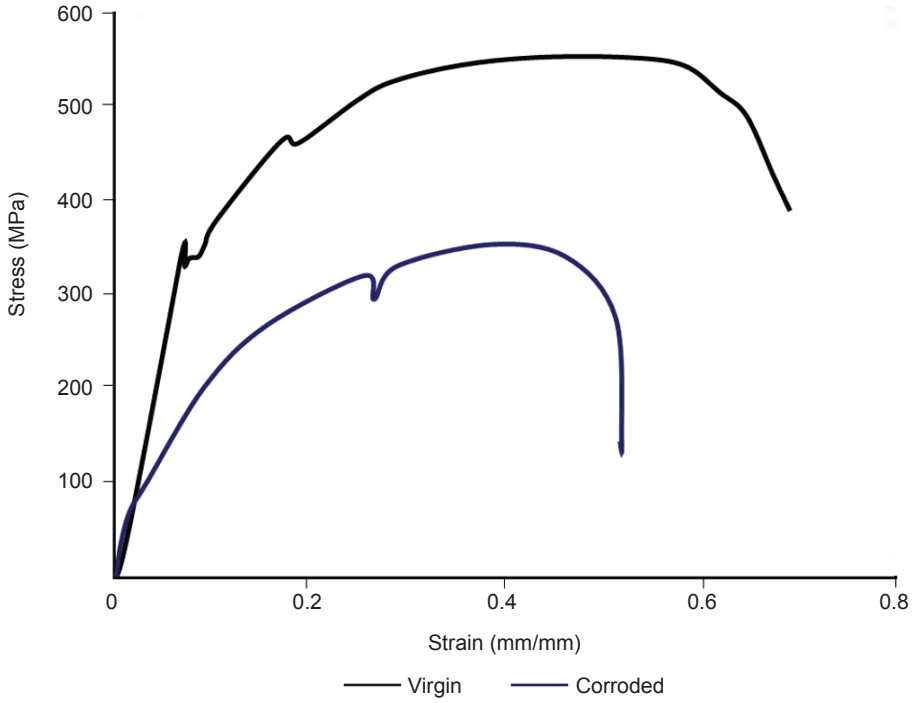

Figure 6. The load displacement curve and damaged specimen.

TABLE 6. THE SPECIMEN DIMENSION AND TENSILE TEST RESULTS

Specimen label	Thickness (mm)	Width (mm)	Maximum load (kN)	Tensile stress at maximum load (MPa)	Tensile strain at maximum load (mm/mm)	Tensile extension at maximum load (mm)
#1	4.4	10.6	16.0	350.4	0.4	11.9
#2	4.4	10.6	16.5	360.3	0.4	12.4
#3	4.4	10.6	17.0	370.2	0.4	12.9

CONCLUSION

In conclusion, this study focused on the impact of B100 biodiesel corrosion on carbon steel storage tanks. The corrosion testing results revealed significant weight and thickness loss in the carbon steel specimens after 15 years of immersion in biodiesel. The UTM results indicated a substantial decrease in corrosion resistance following exposure to B100 biodiesel. SEM and EDS analyses revealed the presence of rust compounds on the specimen surfaces. Tensile test results demonstrated the significant influence of B100 biodiesel corrosion on the mechanical properties of the specimens. These findings highlight the substantial impact of B100 biodiesel corrosion on the performance and reliability of carbon steel storage tanks, emphasising the need for further research in developing effective corrosion prevention and mitigation strategies. It can be suggested that future work should focus on developing more advanced corrosion mitigation and prevention strategies, specifically tailored to the unique challenges posed by biodiesel. It also recommends exploring the efficacy of different materials and coatings, such as glass fibre reinforced polymers (GFRP), to enhance the longevity and reliability of storage tanks instead of a total shell plate replacement. The limitations of the current study include its relatively narrow scope on a specific type of carbon steel and the conditions under which the tests were conducted, which may not fully replicate all operational environments, such as biodiesel blends, exposure time, and temperature. The new knowledge contributed by this study includes detailed insights into the corrosion mechanisms of 15 years old ASME SA 516 Grade 70 carbon steel immersed in a B100 biodiesel environment, highlighting the critical need for industry- and product-specific maintenance and inspection systems.

REFERENCES

Aatola, H., Larmi, M., Sarjovaara, T., & Mikkonen, S. (2009). Hydrotreated vegetable oil (HVO) as a renewable diesel fuel: Trade-off between NO_x, particulate emission, and fuel consumption of a heavy duty engine. *SAE International Journal of Engines*, *1*(1), 1251–1262.

Alam, M., Zafar, F., Ghosal, A., & Ahmed, M. (2022). Formulation of silica-based corn oil transformed polyester acryl amide-phenol formaldehyde corrosion resistant coating material. *Journal of Applied Polymer Science*, *139*(7). https://doi.org/10.1002/app.51651

American Petroleum Institute. (2014). *API Standard 653. Tank inspection, repair, alteration, and reconstruction*.

Arunkumar, T., Sunitha, S., Theerthagiri, J., Jeevagan, J., Anish, M., & Tatarchuk, T. (2018). Effect of polyurea coating on corrosion resistance over mild steel and aluminium substrates for liquid storage applications. *Molecular Crystals and Liquid Crystals*, *670*(1), 60–73. https://doi.org/10.1080/15421406.2018.1542065

Atikpo, E., Aigbodion, V. S., & Von Kallon, D. V. (2022). $CaCO_3$-derived from eggshell waste for improving the corrosion resistance of zinc composite coating on mild steel for biodiesel storage tank. *Chemistry Data Collections*, *37*, Article 100794. https://doi.org/10.1016/J.CDC.2021.100794

Bacha, J., Freel, J., Gibbs, A., Gibbs, L., Hemighaus, G., Hoekman, K., Horn, J., Ingham, M., Jossens, L., Kohler, D., Lesnini, D., McGeehan, J., Nikanjam, M., Olsen, E., Organ, R., Scott, B., Sztenderowicz, M., Tiedemann, A., Walker, C., . . . Mills, J. (2007). *Diesel fuels technical review*. Chevron Corporation. https://www.chevron.com/-/media/chevron/operations/documents/diesel-fuel-tech-review.pdf

Batista, C. E. D., Fabris, J. D., Cavalcante, L. C. D., Ferraz, V. P., Andrade, B. C., Ardisson, J. D., De Lemos, L. R., & Damasceno, S. M. (2019). Monitoring the composition in esters of the biodiesel from the macauba (*Acrocomia Aculeata* (Jacq.) Lodd. Ex Mart.) kernel oil put in direct contact with carbon steel and galvanized carbon steel. *Química Nova*, *42*(4), 387–396. https://doi.org/10.21577/0100-4042.20170356

Chen, B. X., & Sun, J. P. (2022). A radiative cooling, anti-corrosion multifunctional composite coating derived from Jatropha (*Jatropha curcas* L.) oil. *Polymer Engineering & Science*, *62*(11), 3652–3661. https://doi.org/10.1002/pen.26134

Cursaru, D. L., Nassreddine, S., Riachi, B., Neagu, M., Mihai, S., Matei, D., & Branoiu, G. (2018). Impact of moisture on the corrosion behavior of copper and mild carbon steel in corn biodiesel. *Corrosion Reviews*, *36*(6), 559–574. https://doi.org/10.1515/corrrev-2018-0015

Dharma, S., Silitonga, A. S., Shamsuddin, A. H., Sebayang, A. H., Milano, J., Sebayang, R., Sarjianto, Ibrahim, H., Bahri, N., Ginting, B., & Damanik, N. (2023). Properties and corrosion behaviors of mild steel in biodiesel-diesel blends. *Energy Sources, Part A: Recovery, Utilization, and Environmental Effects*, *45*(2), 3887–3899. https://doi.org/10.1080/15567036.2019.1668883

Diaz-Ballote, L., & Genesca, J. (2021). Effect of the free water content in biodiesel on the corrosion of copper and AISI 1045 steel: An approach using the biodiesel/KOH-solution interface. *Anal Bioanalytical Electrochemistry*, *13*(2), 202–213.

Diaz-Ballote, L., Maldonado-Lopez, L., San-Pedro, L., Hernandez-Nunez, E., & Genesca, J. (2022). Glycerol and malonic acid as corrosion inhibitors as seen through the density functional theory perspective. *Journal of the Serbian Chemical Society*, *87*(7-8), 845–856. https://doi.org/10.2298/JSC211201012D

Fazal, M. A., Haseeb, A. S. M. A., & Masjuki, H. H. (2011). Effect of temperature on the corrosion behavior of mild steel upon exposure to palm biodiesel. *Energy*, *36*(5), 3328–3334. https://doi.org/10.1016/J.ENERGY.2011.03.028

Fazal, M. A., Haseeb, A. S. M. A., & Masjuki, H. H. (2012). Degradation of automotive materials in palm biodiesel. *Energy*, *401*(1), 76–83. https://doi.org/10.1016/J.ENERGY.2012.02.026

Fazal, M. A., Haseeb, A. S. M. A., & Masjuki, H. H. (2013). Corrosion mechanism of copper in palm biodiesel. *Corrosion Science*, *67*, 50–59. https://doi.org/10.1016/J.CORSCI.2012.10.006

Fazal, M. A., Suhaila, N. R., Haseeb, A., & Rubaiee, S. (2018). Sustainability of additive-doped biodiesel: Analysis of its aggressiveness toward metal corrosion. *Journal of Cleaner Production*, *181*, 508–516. https://doi.org/10.1016/j.jclepro.2018.01.248

Fazal, M. A., Rubaiee, S., & Al-Zahrani, A. (2019). Overview of the interactions between automotive

materials and biodiesel obtained from different feedstocks. *Fuel Processing Technology*, *196*. https://doi.org/10.1016/j.fuproc.2019.106178

Fernandes, D. M., Squissato, A. L., Lima, A. F., Richter, E. M., & Munoz, R. A. A. (2019). Corrosive character of *Moringa oleifera* Lam biodiesel exposed to carbon steel under simulated storage conditions. *Renewable Energy*, *139*, 1263–1271. https://doi.org/10.1016/j.renene.2019.03.034

Fernandes, F. D., Ferreira, L. M., & Da Silva, M. (2021a). Application of *Psidium guajava* L. leaf extract as a green corrosion inhibitor in biodiesel: Biofilm formation and encrustation. *Applied Surface Science Advances*, *6*, Article 100185. https://doi.org/10.1016/j.apsadv.2021.100185

Fernandes, F. D., Ferreira, L. M., & Da Silva, M. (2021b). Evaluation of the corrosion inhibitory effect of the ecofriendily additive of *Terminalia Catappa* leaf extract added to soybean oil biodiesel in contact with zinc and carbon steel 1020. *Journal of Cleaner Production*, *321*, Article 128863. https://doi.org/10.1016/j.jclepro.2021.128863

Gunstone, F. (2009). *The chemistry of oils and fats: Sources, composition, properties and uses*. John Wiley & Sons.

Jerome, D. M., & Ross, C. A. (1997). Simulation of the dynamic response of concrete beams externally reinforced with carbon-fiber reinforced plastic. *Computers & Structures*, *64*(5-6), 1129–1153.

Jiang, L., He, C., Fu, J., & Xu, D. (2019). Enhancement of wear and corrosion resistance of polyvinyl chloride/sorghum straw-based composites in cyclic sea water and acid rain conditions. *Construction and Building Materials*, *223*, 133–141. https://doi.org/10.1016/j.conbuildmat.2019.06.216

Kardak, A. A., & Sinclair, G. B. (2020). Stress concentration factors for ASTM E8/E8M-16a standard round specimens for tension testing. *Journal of Testing and Evaluation*, *48*(1), 711–719. https://doi.org/10.1520/JTE20190549

Komariah, L. N., Arita, S., Prianda, B. E., & Dewi, T. K. (2021). Technical assessment of biodiesel storage tank: A corrosion case study. *Journal of King Saud University - Engineering Sciences*. https://doi.org/10.1016/j.jksues.2021.03.016

Kugelmeier, C. L., Monteiro, M. R., Da Silva, R., Kuri, S. E., Sordi, V. L., & Della Rovere, C. A. (2021). Corrosion behavior of carbon steel, stainless steel, aluminum and copper upon exposure to biodiesel blended with petrodiesel. *Energy*, *226*, Article 120344. https://doi.org/10.1016/j.energy.2021.120344

Martins, L. F., Cubides-Roman, D. C., da Silveira, V. C., Aquije, G., Romao, W., Dos Santos, R. B., Neto, A. C., & Lacerda, V. (2020). Synthesis of new phenolic-Schiff base and its application as antioxidant in soybean biodiesel and corrosion inhibitor in AISI 1020 carbon steel. *Journal of the Brazilian Chemical Society*, *31*(3), 556–565. https://doi.org/10.21577/0103-5053.20190217

Maru, M. M., Lucchese, M. M., Legnani, C., Quirino, W. G., Balbo, A., Aranha, I. B., Costa, L. T., Vilani, C., De Sena, L. Á., & Damasceno, J. C. (2009). Biodiesel compatibility with carbon steel and HDPE parts. *Fuel Processing Technology*, *90*(9), 1175–1182. https://doi.org/10.1016/j.fuproc.2009.05.014

Nguyen, X. P., & Vu, H. N. (2019). Corrosion of the metal parts of diesel engines in biodiesel-based fuels. *International Journal of Renewable Energy Development*, *8*(2), 119–132. https://doi.org/10.14710/ijred.8.2.119-132

Ouarga, A., Lebaz, N., Tarhini, M., Noukrati, H., Barroug, A., & Elaissari, A. (2022). Towards smart self-healing coatings: Advances in micro/nano-encapsulation processes as carriers for anti-corrosion coatings development. *Journal of Molecular Liquids*, *361*, Article 118862. https://doi.org/10.1016/j.molliq.2022.118862

Parveez, G. K. A., Tarmizi, A. H. A., Sundram, S., Loh, S. K., Ong-Abdullah, M., Palam, K. D. P., Salleh, K. M., Ishak, S. M., & Idris, Z. (2021). Oil palm economic performance in Malaysia and R&D progress in 2020. *Journal of Oil Palm Research*, *33*(2), 181–214. https://doi.org/10.21894/jopr.2021.0026

Parliament of Malaysia. (1967). *Laws of Malaysia Act 235 Customs Act 1967*. Government of Malaysia.

Patil, C. K., Jirimali, H. D., Paradeshi, J. S., Chaudhari, B. L., Alagi, P. K., Hong, S. C., & Gite, V. V. (2018). Synthesis of biobased polyols using algae oil for multifunctional polyurethane coatings. *Green Materials*, *6*(4), 165–177. https://doi.org/10.1680/jgrma.18.00046

Purschke, M. (2013). *ISO 9712: 2012 - A worldwide standard for qualification and certification of NDT personnel - A European view*. Non-Destructive Testing-Australia.

Pusparizkita, Y. M., Schmahl, W. W., Setiadi, T., Ilsemann, B., Reich, M., Devianto, H., & Harimawan, A. (2020). Evaluation of bio-corrosion on carbon steel by *Bacillus megaterium* in biodiesel and diesel oil mixture. *Journal of Engineering and Technological Science*, *52*(3), 370–384. https://doi.org/10.5614/j.eng.technol.sci.2020.52.3.5

Rocha, J. G., Dos Santos, M. D. R., Madeira, F. B., Rocha, S., Bauerfeldt, G. F., Da Silva, W. L. G., Salomao, A. A., & Tubino, M. (2019). Influence of fatty acid methyl ester composition, acid value, and water content on metallic copper corrosion caused by biodiesel. *Journal of the Brazilian Chemical Society*, *30*(8), 1751–1761. https://doi.org/10.21577/0103-5053.20190078

Samuel, O. D., & Gulum, M. (2019a). Mechanical and corrosion properties of brass exposed to waste sunflower oil biodiesel-diesel fuel blends. *Chemical Engineering Communications*, *206*(5), 682–694. https://doi.org/10.1080/00986445.2018.1519508

Serqueira, D. S., Pereira, J. F. S., Squissato, A. L., Rodrigues, M. A., Lima, R. C., Faria, A. M., Richter, E. M., & Munoz, R. A. A. (2021). Oxidative stability and corrosivity of biodiesel produced from residual cooking oil exposed to copper and carbon steel under simulated storage conditions: Dual effect of antioxidants. *Renewable Energy*, *164*, 1485–1495. https://doi.org/10.1016/j.renene.2020.10.097

Sgroi, M., Bollito, G., Saracco, G., & Specchia, S. (2005). BIOFEAT: Biodiesel fuel processor for a vehicle fuel cell auxiliary power unit: Study of the feed system. *Journal of Power Sources*, *149*, 8–14. https://doi.org/10.1016/j.jpowsour.2004.12.059

Touazi, Y., Abdi, A., Leshaf, A., & Khimeche, K. (2020). Influence of heat treatment of iron oxide on its effectiveness as anticorrosion pigment in epoxy based coatings. *Progress in Organic Coatings*, *139*, Article 105458. https://doi.org/10.1016/j.porgcoat.2019.105458

Wei, Z., Zandi, Y., Gholizadeh, M., Selmi, A., Roco-Videla, A., & Konbr, U. (2021). On the optimization of building energy, material, and economic management using soft computing. *Advances in Concrete Construction*, *11*(5), 455–468. https://doi.org/10.12989/acc.2021.11.6.455

Yi, C., Rostron, P., Vahdati, N., Gunister, E., & Alfantazi, A. (2018). Curing kinetics and mechanical properties of epoxy based coatings: The influence of added solvent. *Progress in Organic Coatings*, *124*, 165–174. https://doi.org/10.1016/j.porgcoat.2018.08.009

Yung, C. L., Jalil, N., Miyamoto, M., Sakamoto, S., Maruyama, K., Loh, S. K., & Lim, W. S. (2018). Compatibility of terne sheet with palm biodiesel blends. *Journal of Oil Palm Research*, *30*(4), 655–665. https://doi.org/10.21894/jopr.2018.0036

Yusoff, M. N. A. M., Zulkifli, N. W. M., Sukiman, N. L., Chyuan, O. H., Hassan, M. H., Hasnul, M. H., Zulkifli, M. S. A., Abbas, M. M., & Zakaria, M. Z. (2021). Sustainability of palm biodiesel in transportation: A review on biofuel standard, policy and international collaboration between Malaysia and Colombia. *BioEnergy Research*, *14*(1), 43–60. https://doi.org/10.1007/s12155-020-10165-0